SUPPLEMENTARY DATA

Fluorescent biogenic Schiff base compounds of dimethyltin

Navjot Singh[a,b], Neha Srivastav[a], Raghubir Singh[b*], Varinder Kaur[a*], Erica Brendler[c], Jörg Wagler[d], Edwin Kroke[d]

[a]Department of Chemistry, Panjab University, Sector-14, Chandigarh-160014,

[b]Department of Chemistry, DAV college, Sector 10, Chandigarh-160011

[c]Institut für Analytische Chemie, Technische Universität Bergakademie, Freiberg – 09596 Freiberg, Germany

[d]Institut für Anorganische Chemie, Technische Universität Bergakademie, Freiberg – 09596 Freiberg, Germany

1. Synthesis

1.1. Synthetic procedure for 4. A suspension of Me_2SnO (0.20 g, 1.21 mmol), 2-hydroxy-4-methoxybenzophenone (0.28 g, 1.21 mmol), and alanine (0.11 g, 1.21 mmol), in methanol (60 mL) was heated to reflux in a Dean-stark apparatus for 8 h. Solution was concentrated to one-fifth of its original volume under vacuum and the remaining solvent was removed completely and the product was extracted with chloroform. The chloroform was evaporated to obtain yellow solid, which was washed with ether to remove soluble impurities.

6-Aza-11-methoxy-2,2,5-trimethyl-1,3-dioxa-7-phenyl-2-stannabenzocyclononen-4(5H)-one (4).

Yield (crude product) 40 %. (0.21 g, 0.47 mmol). M.p.: decomposed, 217-220 °C. IR (cm^{-1}): 461 s (υ Sn←N), 548 s (υ Sn–O), 706 s (υ_s Sn–C), 1411 m (υ_s C=O), 1597 s (C=N), 1670 s (υ_{as} C=O). ^{1}H NMR (400 MHz, $CDCl_3$): δ (ppm) 0.69 (s, 3 H, $SnCH_3$, $^2J(^1H\text{-}^{117}Sn)$ = 74 Hz, $^2J(^1H\text{-}^{119}Sn)$ = 77 Hz), 1.01 (s, 3 H, $SnCH_3$ $^2J(^1H\text{-}^{117}Sn)$ = 77 Hz, $^2J(^1H\text{-}^{119}Sn)$ = 80 Hz), 1.33 (d, 3 H, CCH_3[13], $^3J(^1H\text{-}^1H)$ = 7 Hz), 3.80 (s, 3 H, OCH_3), 4.19 (q, 1 H, NCH, $^3J(^1H\text{-}^1H)$ = 7 Hz, $^4J(^1H\text{-}^{117}Sn)$ = 36 Hz, $^4J(^1H\text{-}^{119}Sn)$ = 50 Hz), 6.15 (dd, 1 H^4, $^4J(^1H\text{-}^1H)$ = 3 Hz, $^3J(^1H\text{-}^1H)$ = 9 Hz), 6.53 (d, 1 H^2, $^4J(^1H\text{-}^1H)$ = 3 Hz), 6.62 (d, 1 H^5, $^3J(^1H\text{-}^1H)$ = 9 Hz), 7.12-7.14 (m, 1 H^8), 7.29-7.31 (m, 1 H^{12}), 7.51-7.59 (m, 3 $H^{9,10,11}$), 8.32 (s, 1 H, NH). ^{13}C NMR (100 MHz, $CDCl_3$): δ (ppm) -1.7 (3 H, $SnCH_3$, $^1J(^{13}C\text{-}^{117}Sn)$ = 613 Hz, $^1J(^{13}C\text{-}^{119}Sn)$ = 642 Hz), 1.3 (3 H, $SnCH_3$, $^1J(^{13}C\text{-}^{117}Sn)$ = 652 Hz, $^1J(^{13}C\text{-}^{119}Sn)$ = 689 Hz), 21.3 (C^{13}), 55.5 (OCH_3), 59.4 (NCH), 104.5 (C^2), 107.7 (C^4), 113.9 (C^6), 126.0 (C^{12}), 127.2 (C^8), 129.1 (C^9), 129.2 (C^{11}), 129.9 (C^{10}), 134.3 (C^5), 136.4 (C^7), 166.7 (C^1), 170.5 (C^3), 175.3 (C=N), 179.8 (C=O). ^{119}Sn

NMR (149 MHz, $CDCl_3$): δ (ppm) -163. MS (% relative abundance of m/z assignment): 300 (100) $[L + H]^+$, 322 (3.7) $[L + Na]^+$, 338 (12.7) $[L + K]^+$, 446 (2.4) $[M]^+$, 448 (3.7) $[M + 2H]^+$, 470 (4.0) $[M + Na + H]^+$. $C_{19}H_{21}NO_4Sn$ (446.08): calcd. C 51.16, H 4.75, N 3.14; found C 51.15, H 4.74, N 3.13.

1.2. Synthetic procedure for 2-aminoethanol derivative. A solution of the Schiff base ligand (derived from condensation reaction of 2-aminoethanol and 2-hydroxy-4-methoxybenzophenone in methanol; unpublished) (1.00 g, 3.69 mmol) and dimethyltin(IV) oxide (0.91 g, 3.69 mmol) was refluxed in 50 ml of toluene-methanol (4:6)**.** for 8 h using a Dean-Stark trap. After cooling to room temperature the solvents were evaporated under vacuum to obtain a yellow product. It was washed with hexane, dried and stored under inert atmosphere.

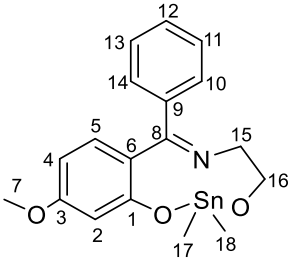

$N[CH_2CH_2O][C(Ph)(OMe\text{-}C_6H_3)O]SnMe_2$:

Yield 75% (1.17 g, 2.79 mmol). M.p. 124-126°C. IR (cm^{-1}): 409 (Sn–N), 559 (Sn–O), 1589 (C=N). ^1H NMR (400 MHz, $CDCl_3$): δ (ppm) 0.66 (s, $6H^{17,18}$, $^2J(^1H\text{-}^{117}Sn)$ = 72.3 Hz, $^2J(^1H\text{-}^{119}Sn)$ = 75.3 Hz), 3.24 (t, $2H^{15}$, $^3J(^1H\text{-}^1H)$ = 5.5 Hz), 3.75 (s, $3H^7$), 3.92 (t, $2H^{16}$, $^3J(^1H\text{-}^1H)$ = 5.5 Hz), 6.05 (dd, $1H^4$, $^4J(^1H\text{-}^1H)$ = 2.5 Hz, $^3J(^1H\text{-}^1H)$ = 9.2 Hz), 6.26 (d, $1H^5$, $^4J(^1H\text{-}^1H)$ = 2.5 Hz), 6.54 (d, $1H^2$, $^3J(^1H\text{-}^1H)$ = 9.2 Hz), 7.22-7.26 (m, $2H^{10,14}$), 7.46-7.55 (m, $3H^{11\text{-}13}$). ^{13}C NMR (75 MHz, $CDCl_3$): δ (ppm) 0.68 ($C^{17,18}$), 21.5 (C^{15}), 55.4 (C^{16}), 60.7 (C^7), 104.4 (C^2), 106.4 (C^4), 114.5 (C^6), 126.3 (C^9), 128.3 (C^{11}), 129.1 (C^{13}), 129.3 (C^{12}), 135.9 (C^{10}), 136.0 (C^{14}), 136.4 (C^5), 165.5 (C^1), 170.4 (C^3), 180.1 (C^8). ^{119}Sn NMR (149 MHz, $CDCl_3$): δ (ppm) -160. MS (% relative abundance of m/z assignment): 272 (100) $[L]^+$, 294 (29.7) $[L + Na]^+$, 544 (6.4) $[M + C_7H_6O_2 + H]^+$, 565 (10.7) $[M – C_{13}H_{14}O – OCH_3 – C_6H_5]^+$, 836 [2M], 852 (3.2) $[2M + NH_3 - H]^+$. $C_{18}H_{21}NO_3Sn$ (418.08): calcd. C, 51.71; H, 5.06; N, 3.35; found C, 51.54; H, 4.99; N, 3.67.

2. Detailed spectra for 1-4

Compound 1

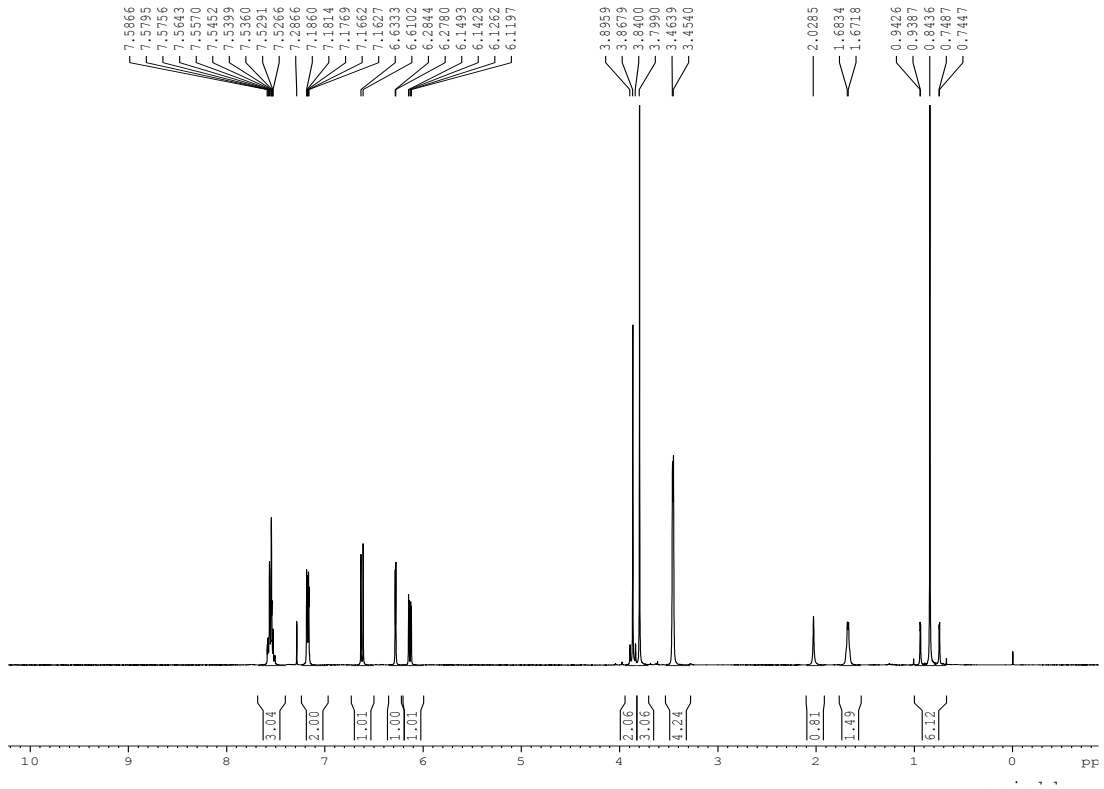

Fig. S1a ^{1}H NMR spectra of compound **1**.

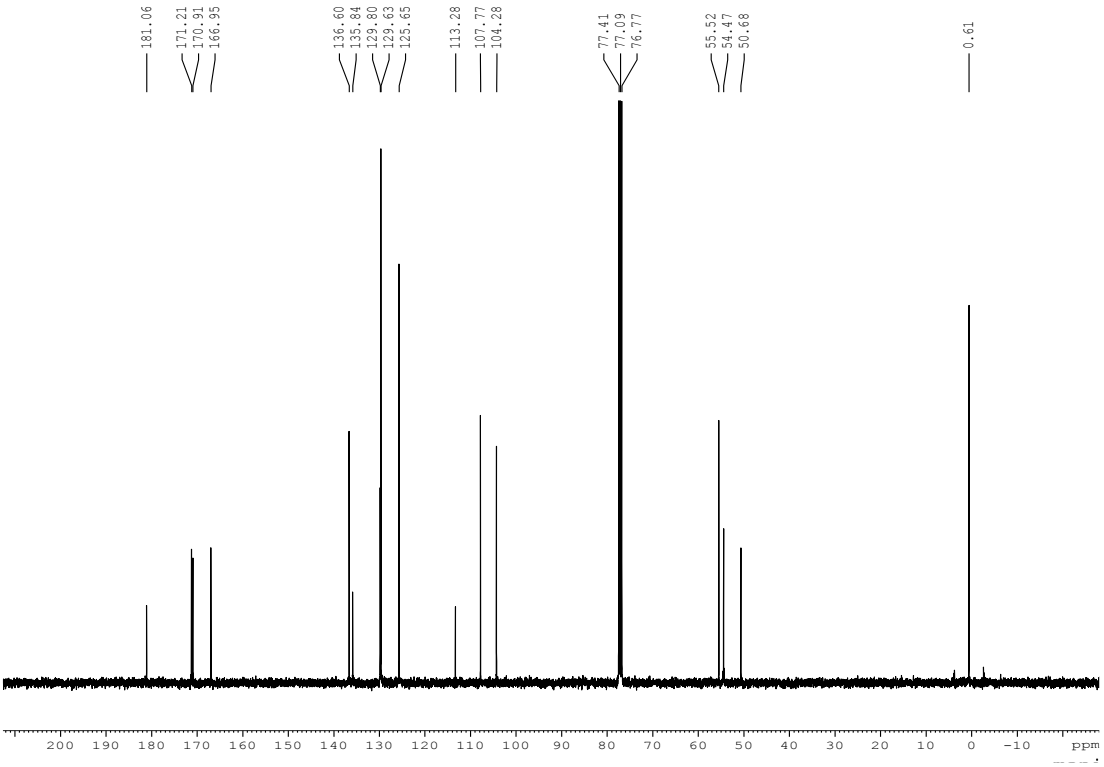

Fig. S1b ^{13}C NMR spectra of compound **1**.

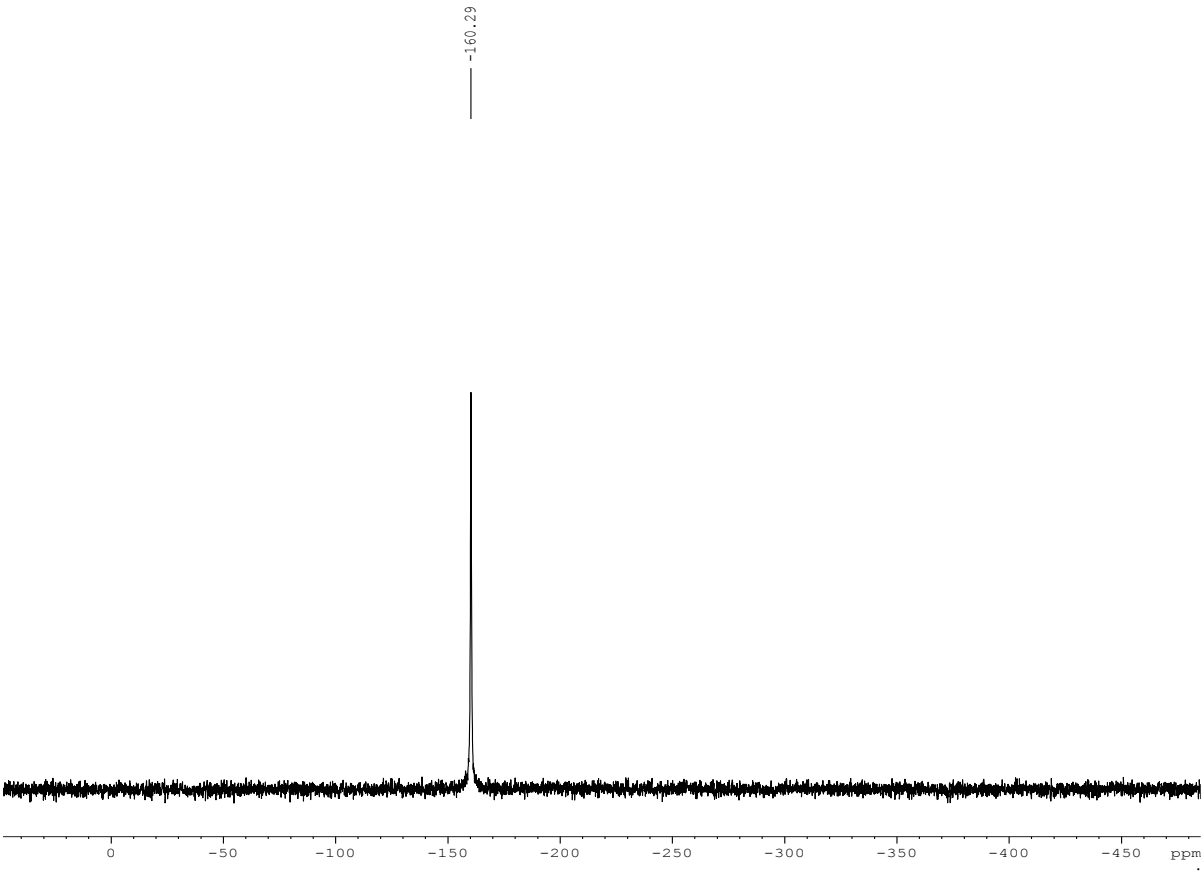

Fig. S1c ^{119}Sn NMR spectra of compound **1**.

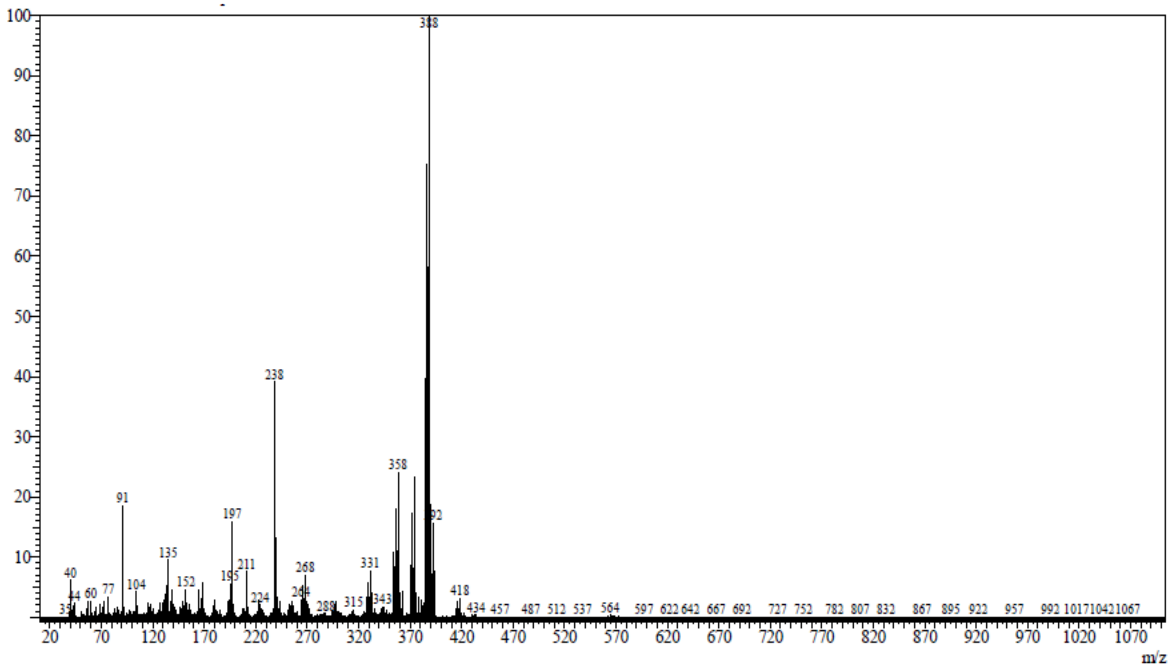

Fig. S1d Mass spectrum of compound **1**.

Compound 2'

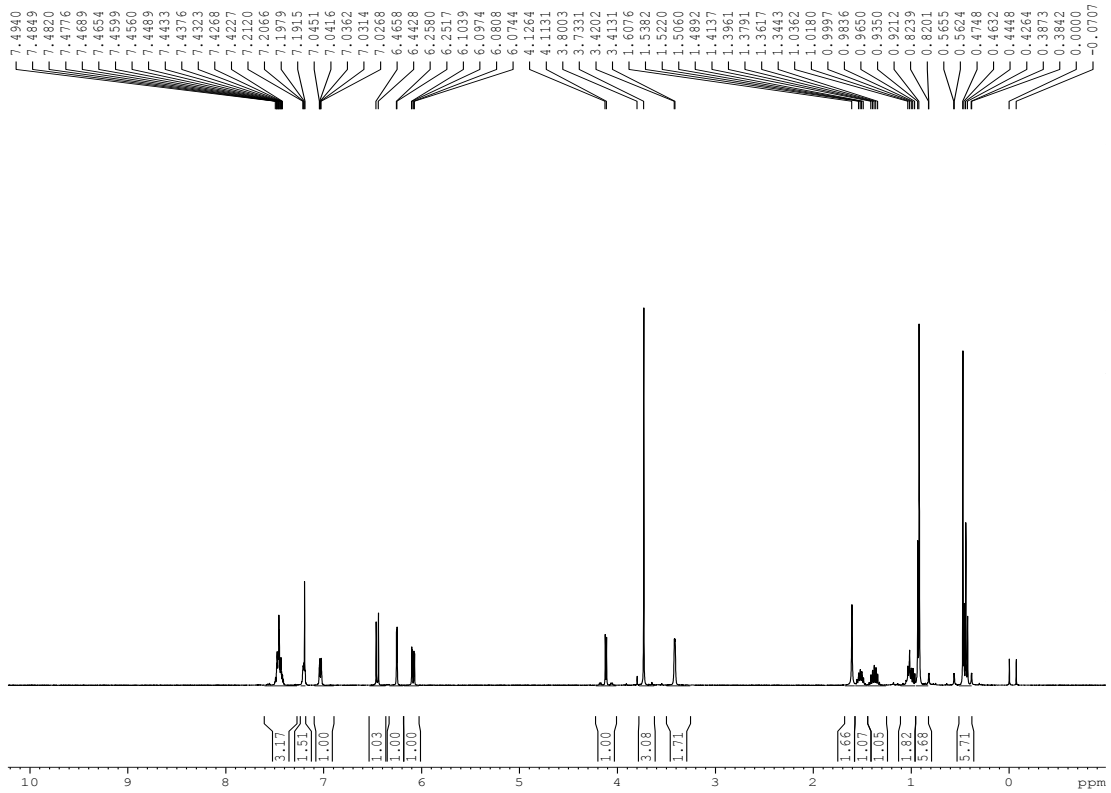

Fig. S2a ^{1}H NMR spectra of compound **2'**.

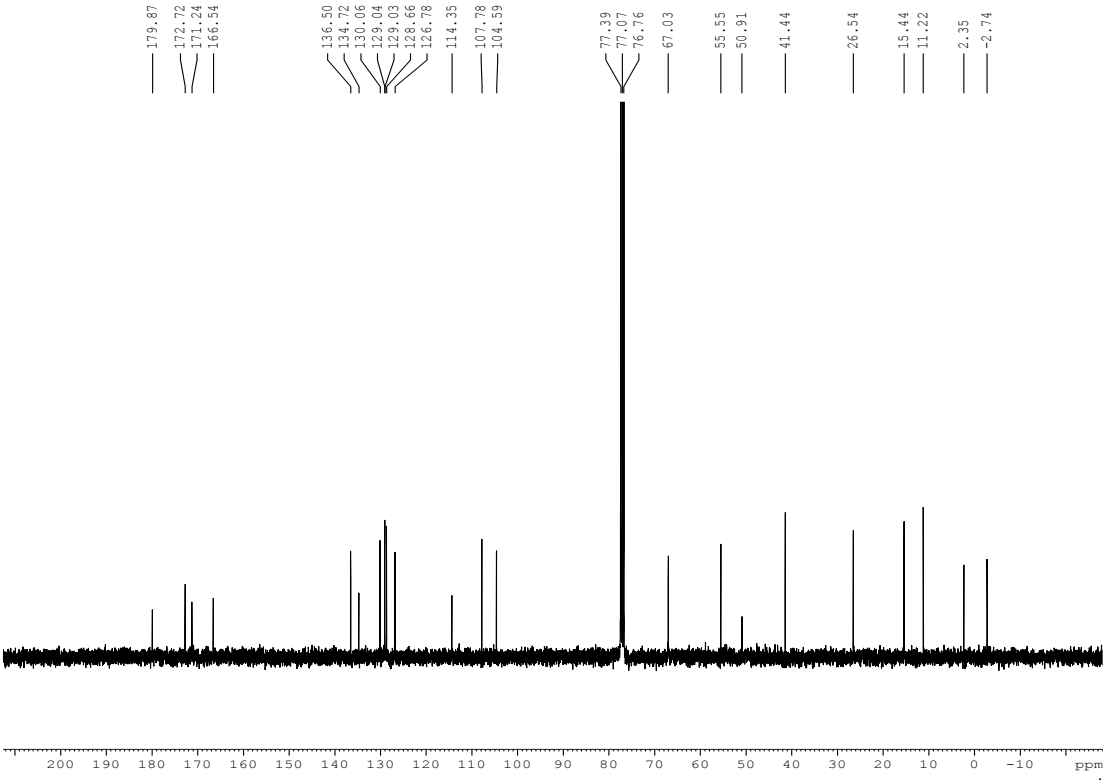

Fig. S2b ^{13}C NMR spectra of compound **2'**.

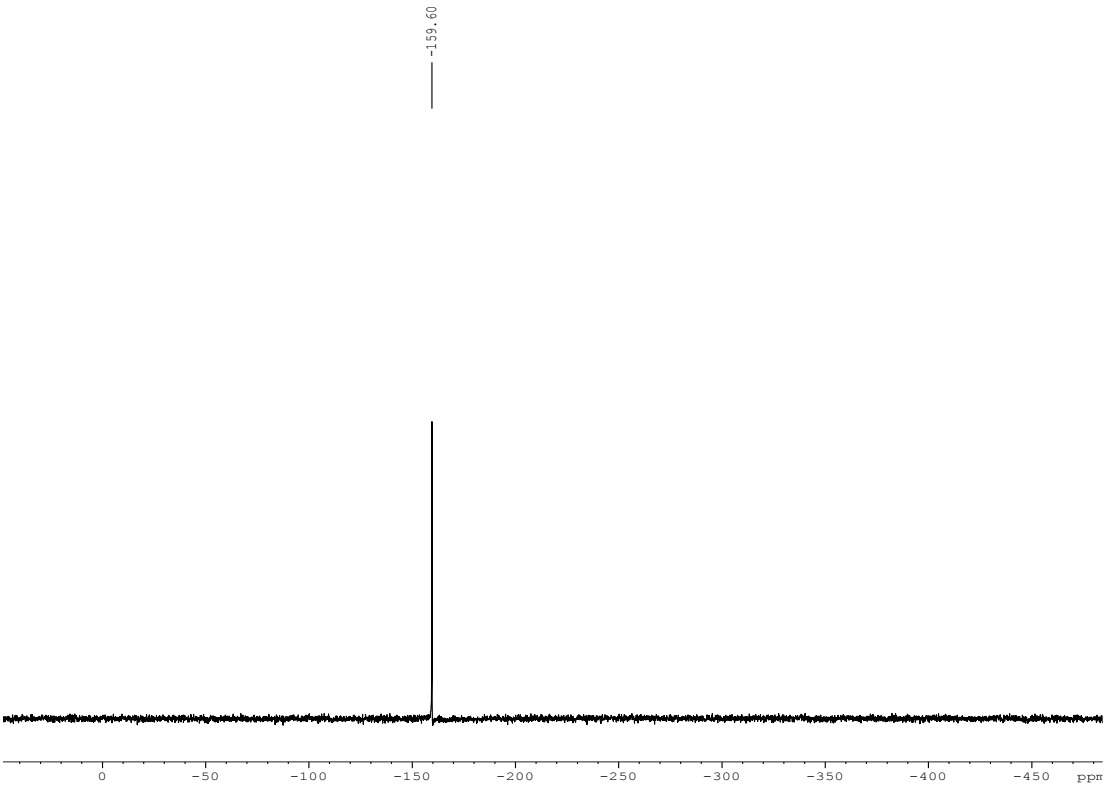

Fig. S2c ^{119}Sn NMR spectra of compound **2'**.

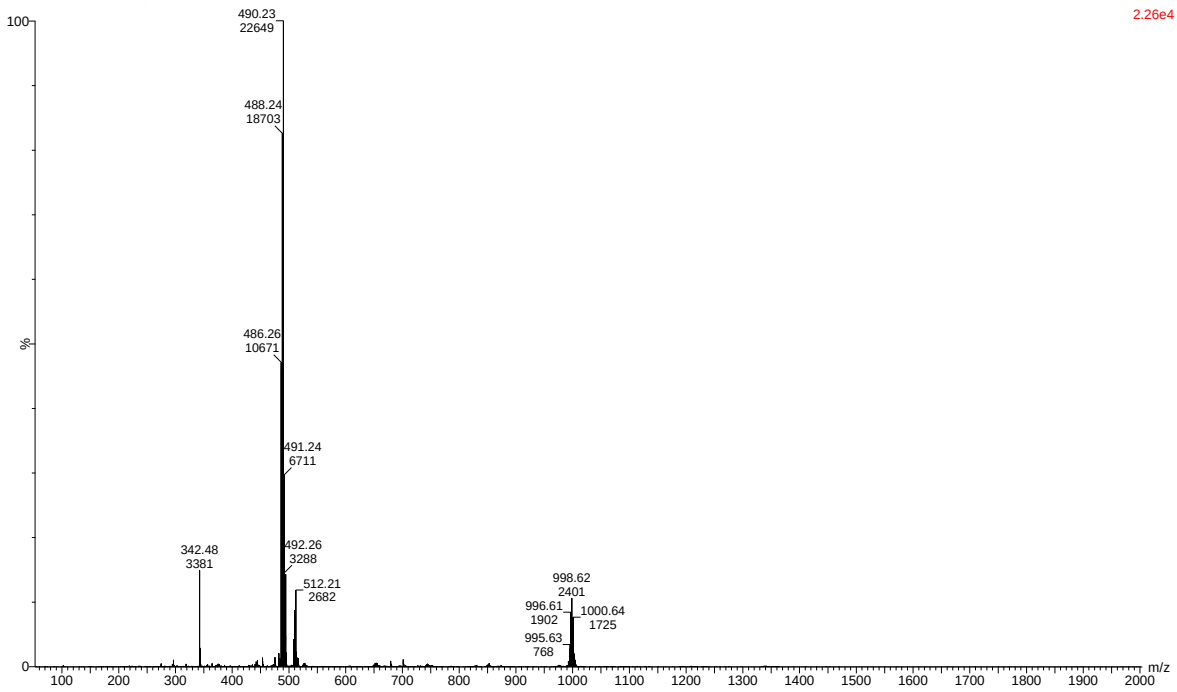

Fig. S2d Mass spectrum of compound **2'**.

Compound 3’

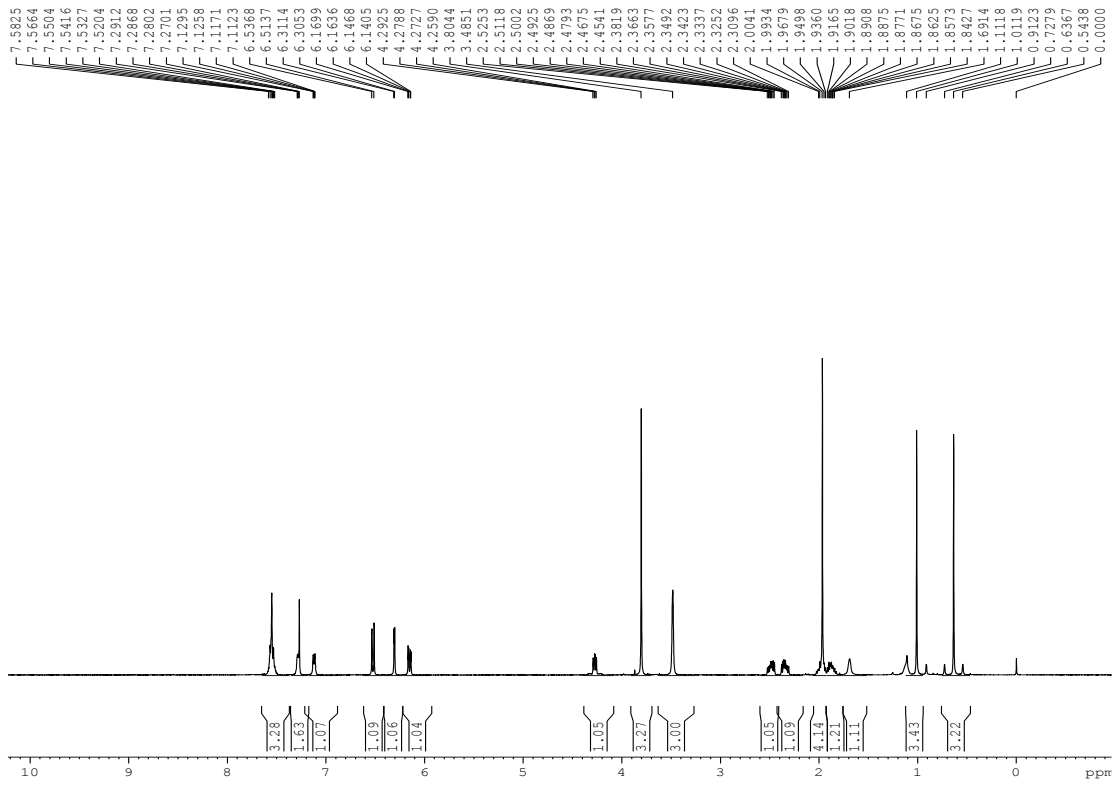

Fig. S3a ^{1}H NMR spectra of compound **3'**.

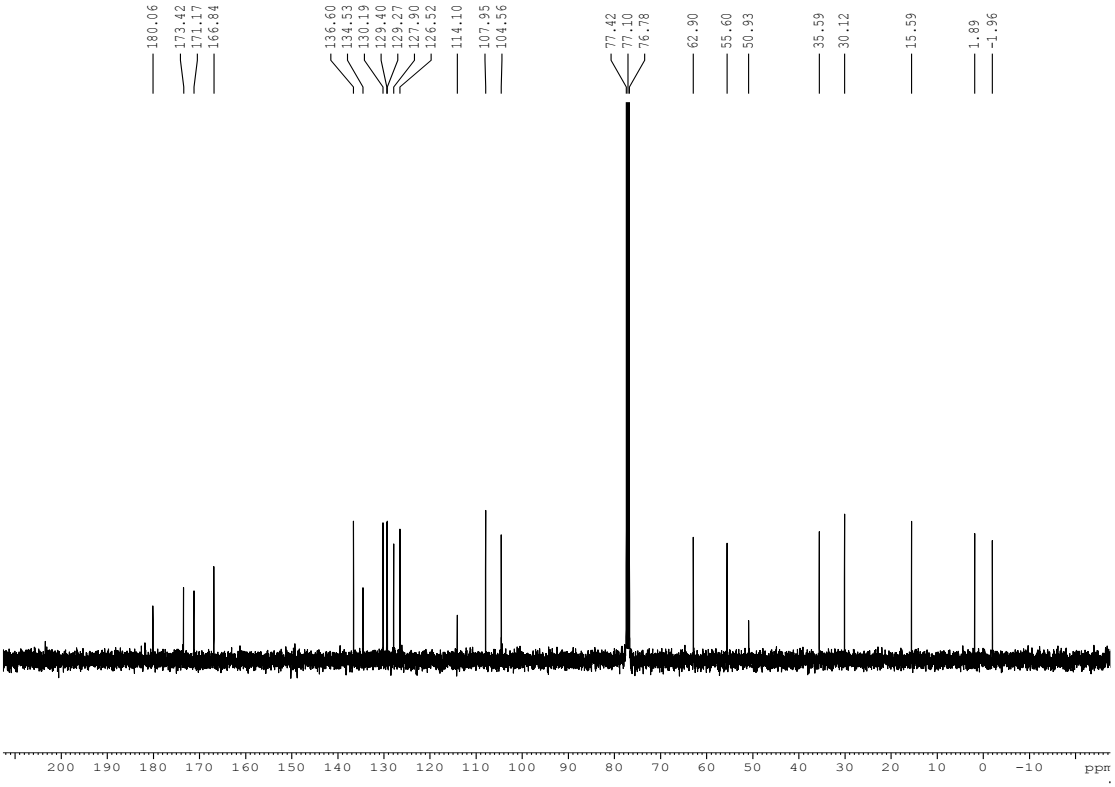

Fig. S3b ^{13}C NMR spectra of compound **3'**.

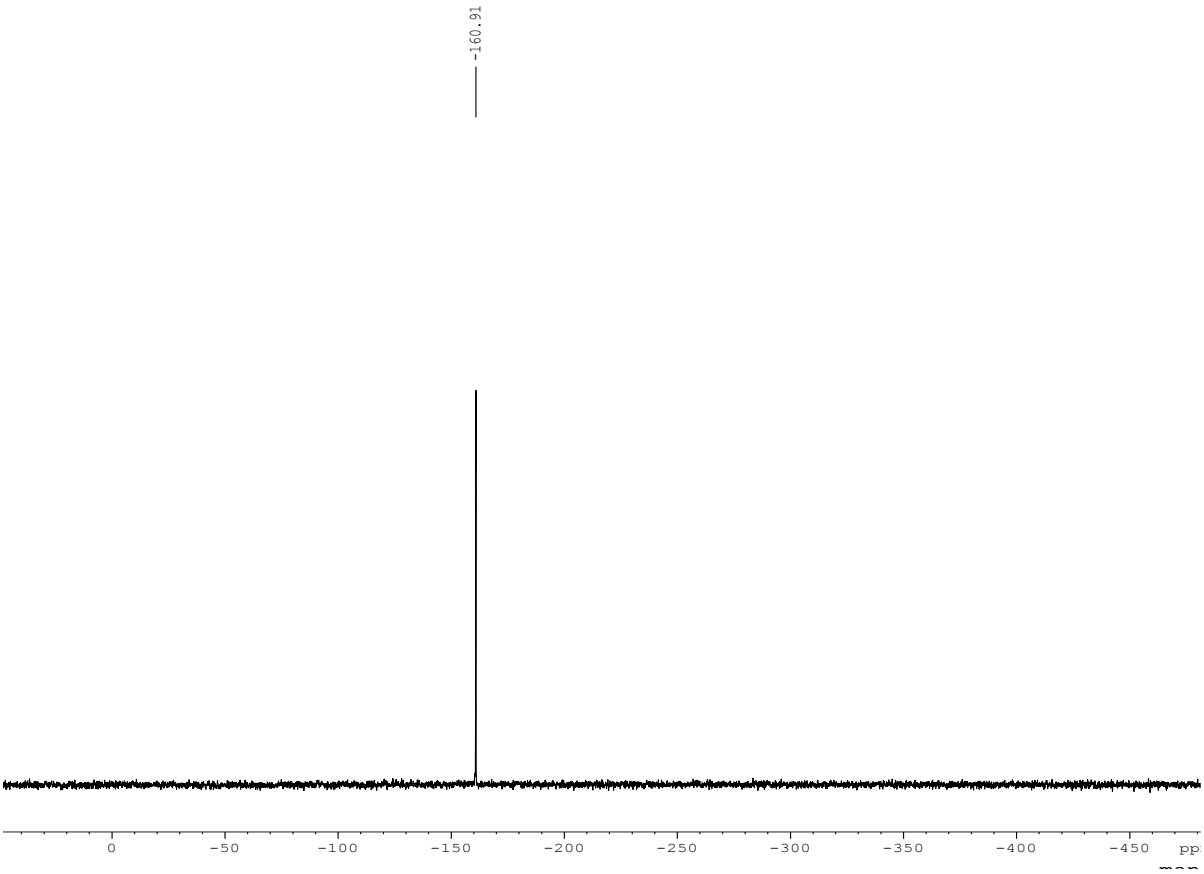

Fig. S3c ^{119}Sn NMR spectra of compound **3'**.

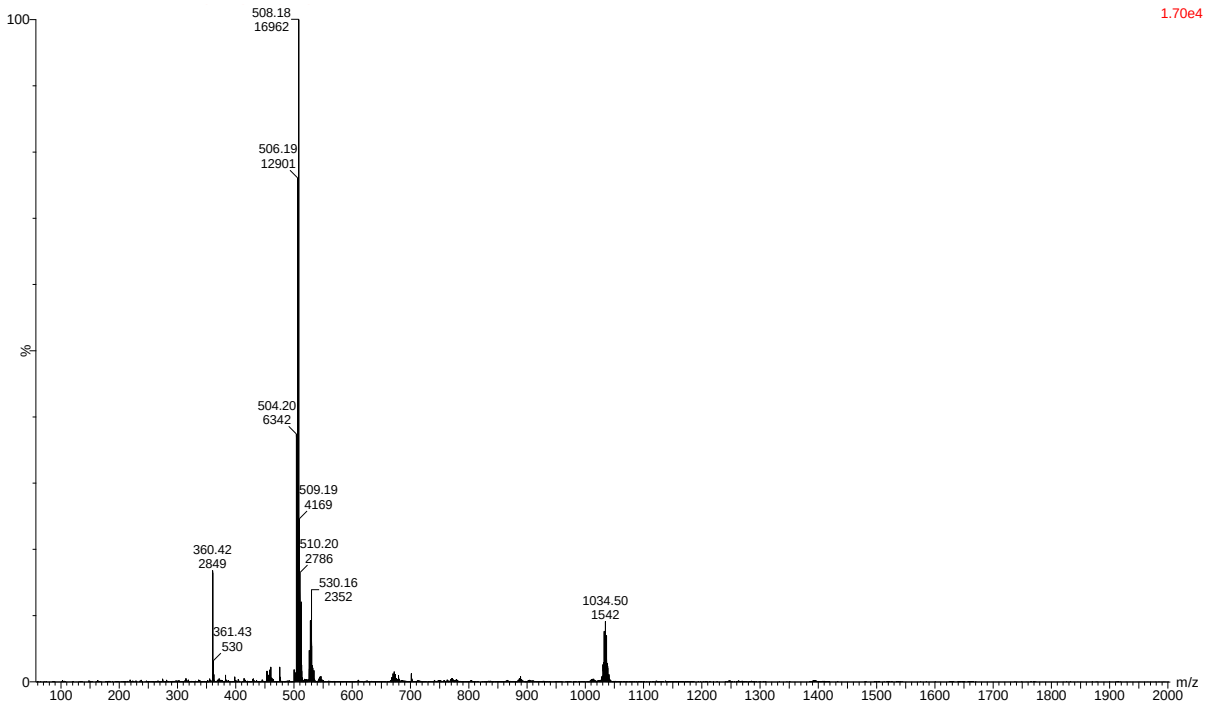

Fig. S3d Mass spectrum of compound **3'**.

Compound 4

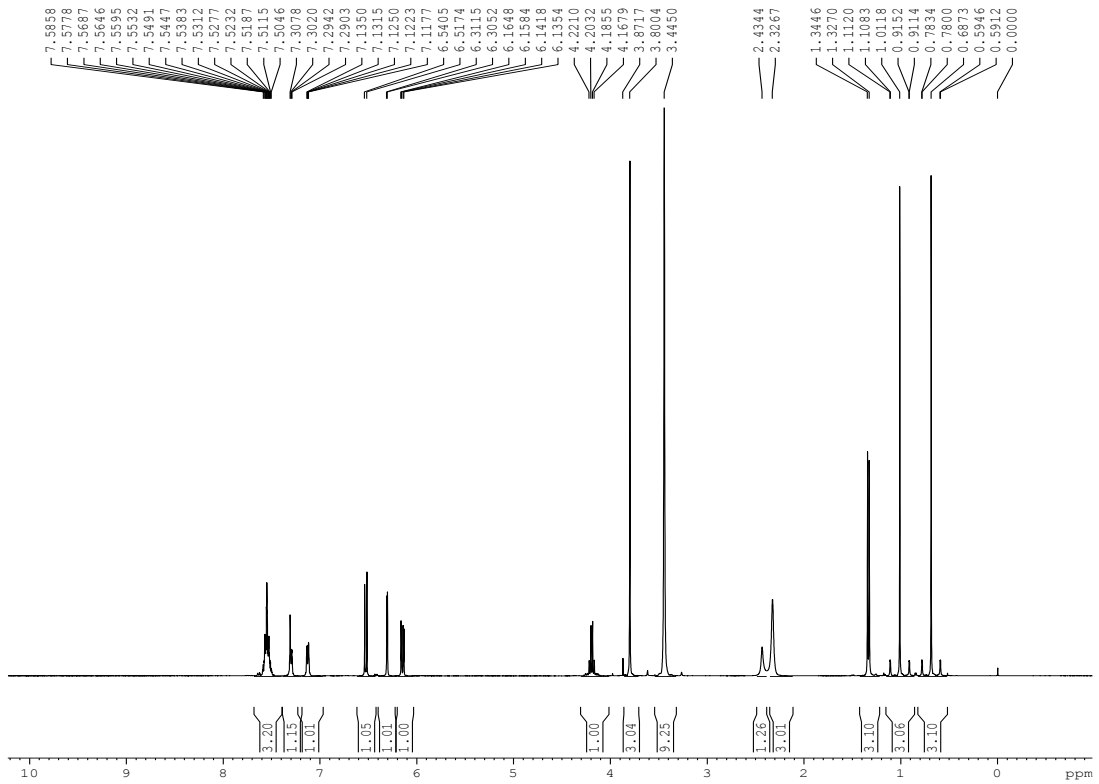

Fig. S4a ^{1}H NMR spectra of compound **4**.

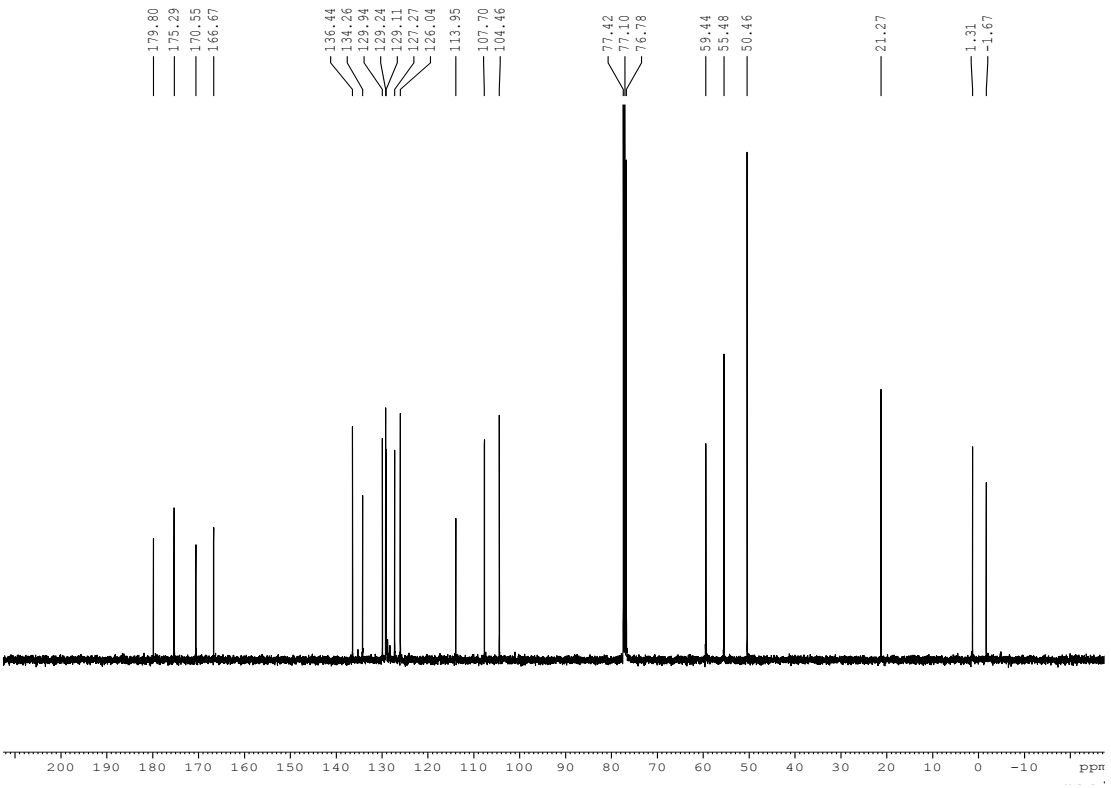

Fig. S4b ^{13}C NMR spectra of compound **4**.

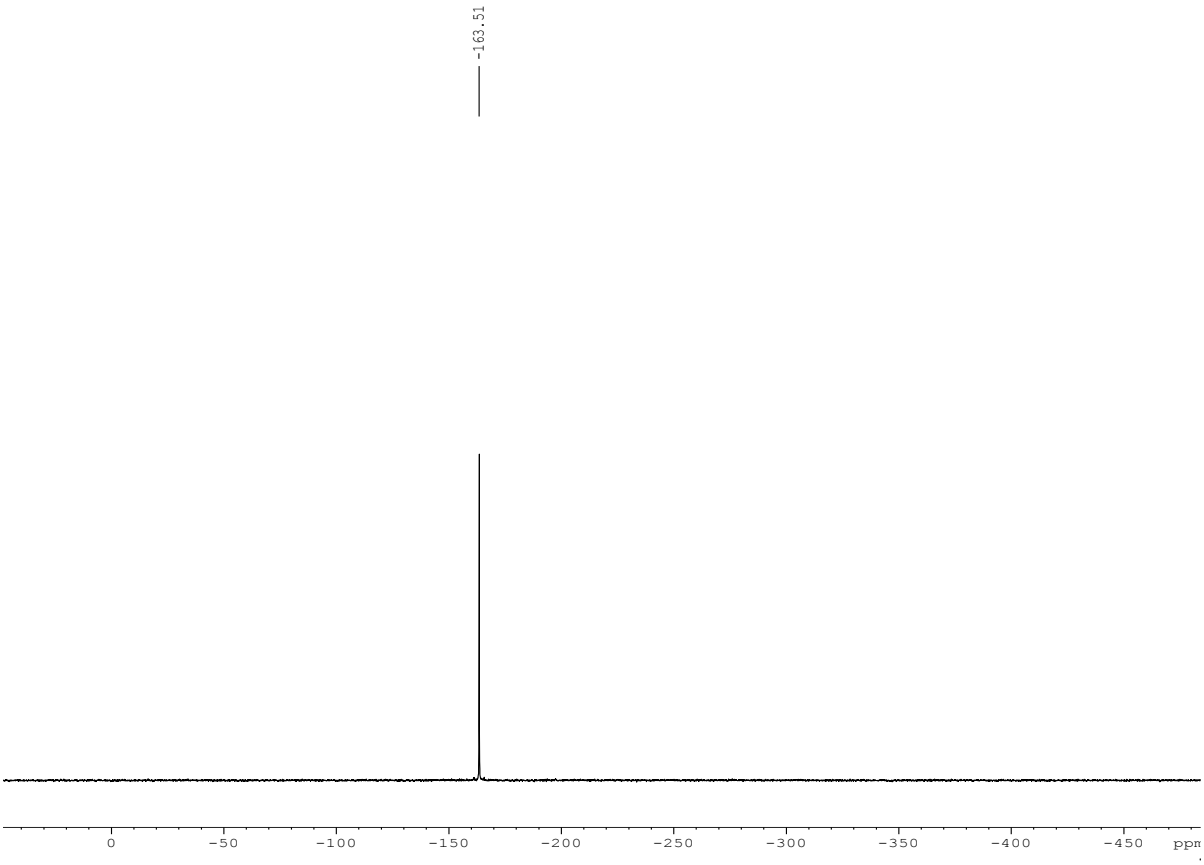

Fig. S4c ^{119}Sn NMR spectra of compound **4**.

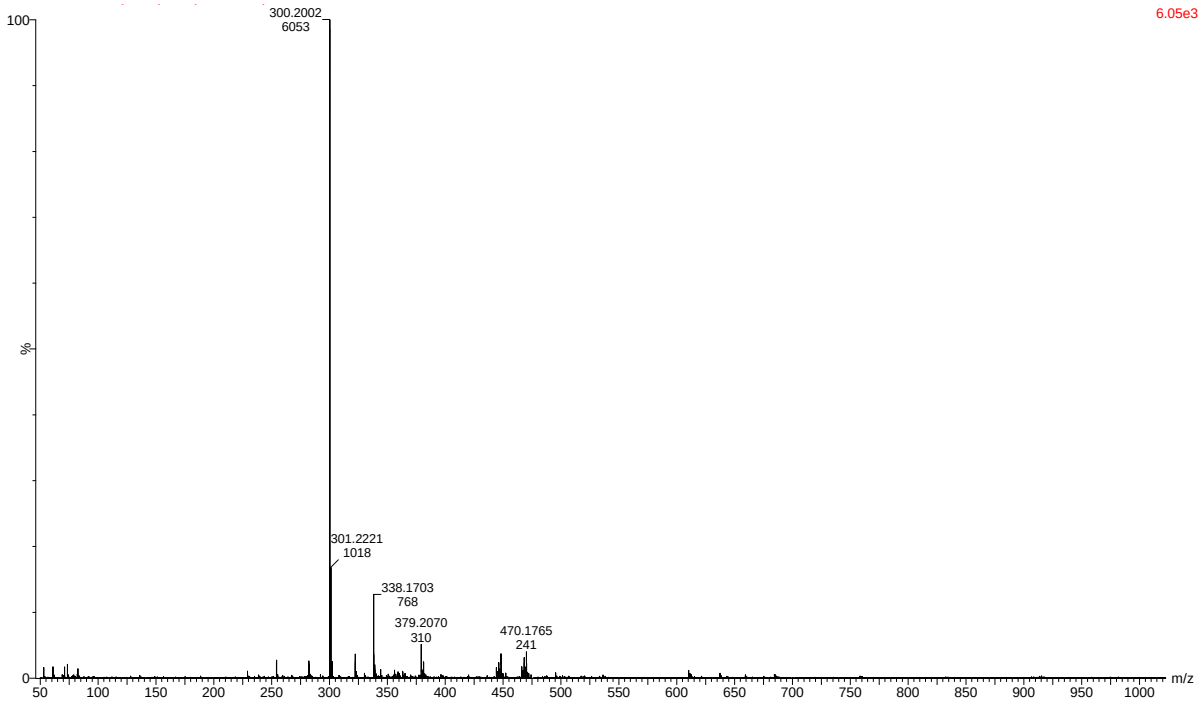

Fig. S4d Mass spectrum of compound **4**.

2-Aminoethanol derivative

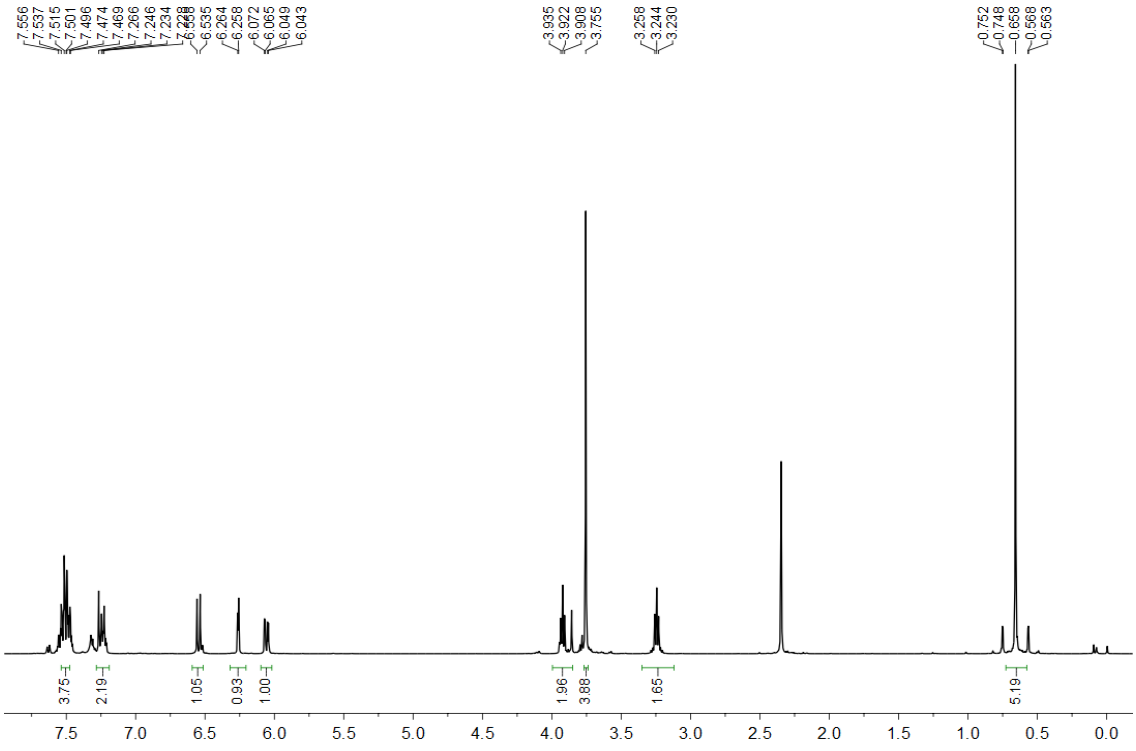

Fig. S5a ^{1}H NMR spectra of 2-aminoethanol analogue.

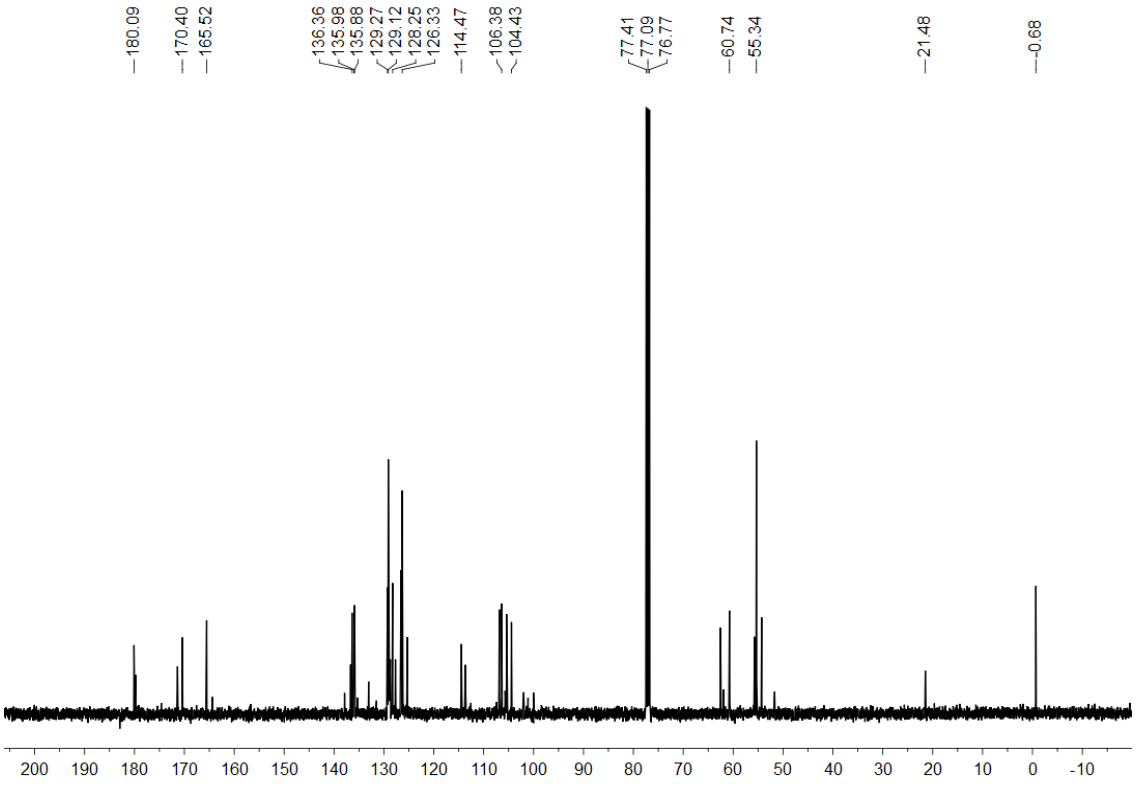

Fig. S5b ^{13}C NMR spectra of 2-aminoethanol analogue.

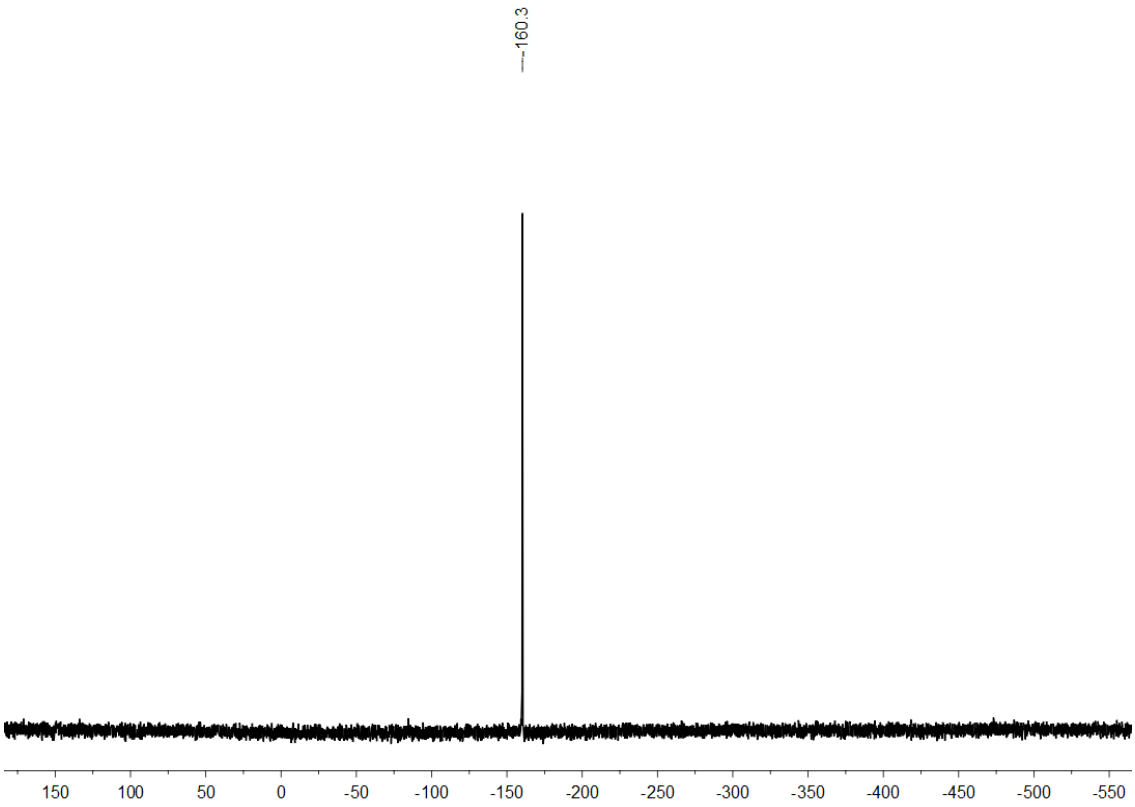

Fig. S5c ^{119}Sn NMR spectra of 2-aminoethanol analogue.

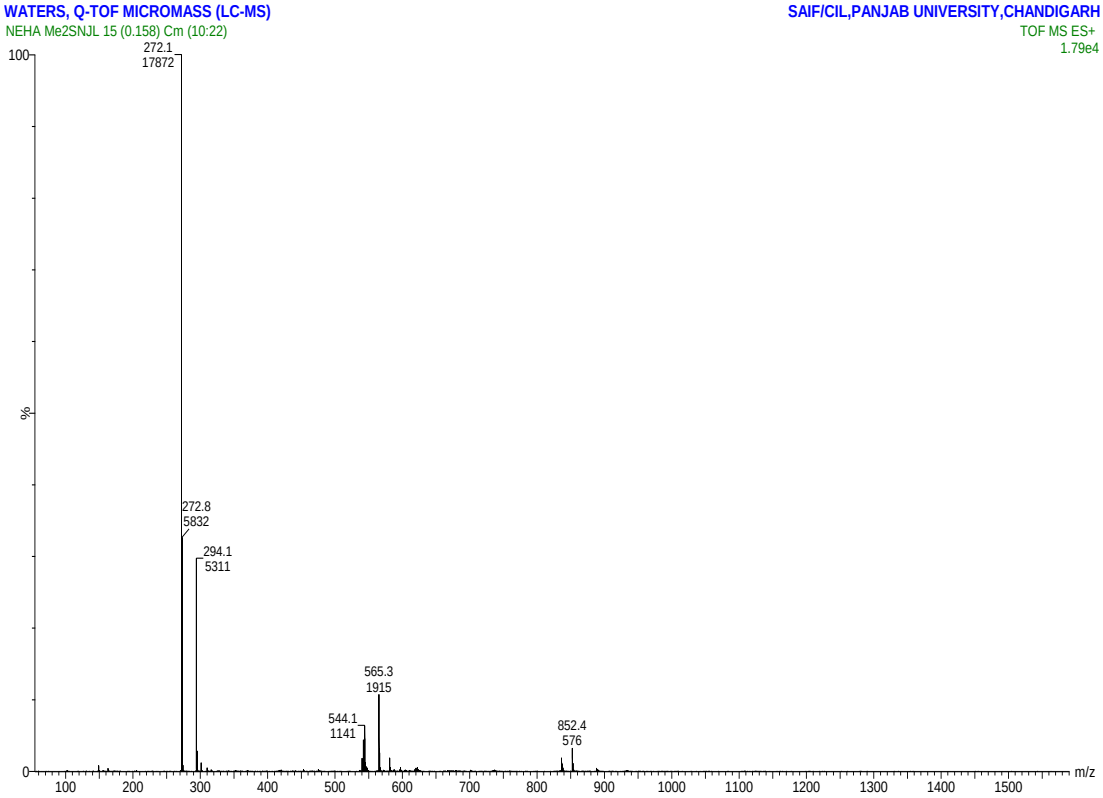

Fig. S5d Mass spectra of 2-aminoethanol analogue.

2. Structural Aspects

Only one signal is observed for solution-state ^{119}Sn NMR spectra (for pentacoordinate Sn atoms).

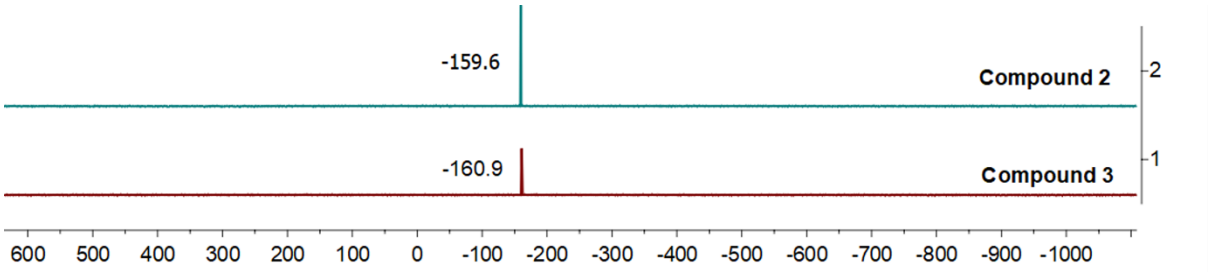

Fig. S6 Solution-state δ ($CDCl_3$ solution, ppm) values for ^{119}Sn NMR spectra of compound **2′** and **3′**.

Table S1 Data of the ^{119}Sn chemical shift anisotropy (CSA) tensors for compounds **2′** and **3′.** The order of the principal values $\delta_{11,22,33}$ as well as span Ω and skew κ are reported according to the Herzfeld-Berger notation. (*For compound **3′** the asymmetric signal at ca. -153 pm was analyzed by deconvolution into two individual contributions.)

compound	**2′**		**3′**		
δ_{iso}	-152.8	-245.9	-152.5*	-152.9*	-244.9
δ_{11}	286.9	235.8	272.5	280.2	245.9
δ_{22}	-50.3	-71.4	-111.6	-49.8	-59.7
δ_{33}	-695.0	-902.2	-615.5	-689.1	-920.9
Ω	981.8	1137.9	887.9	969.4	1166.8
κ	0.31	0.46	0.13	0.32	0.48

3. Description of crystal structure

Table S2: Selected bond lengths (Å) and bond angles (°) for **1.MeOH**.

X-ray Crystal Data					
Sn(1)-O(1)	2.0974(12)	O(1)-Sn(1)-C(17)	98.03(6)	O(1)-Sn(1)-O(5)	74.66(5)
Sn(1)-C(17)	2.0992(18)	O(1)-Sn(1)-C(18)	99.79(6)	C(17)-Sn(1)-O(5)	80.44(6)
Sn(1)-C(18)	2.1039(18)	C(17)-Sn(1)-C(18)	152.32(8)	C(18)-Sn(1)-O(5)	84.06(6)
Sn(1)-N(1)	2.2383(14)	O(1)-Sn(1)-N(1)	78.80(5)	N(1)-Sn(1)-O(5)	153.39(5)
Sn(1)-O(3)	2.3750(12)	C(17)-Sn(1)-N(1)	101.63(7)	O(3)-Sn(1)-O(5)	136.47(4)
Sn(1)-O(5)	2.5533(13)	C(18)-Sn(1)-N(1)	102.49(7)	C(16)-O(3)-Sn(1)	116.60(11)
O(3)-C(16)	1.273(2)	O(1)-Sn(1)-O(3)	148.86(4)	C(19)-O(5)-Sn(1)	122.72(13)

O(4)-C(16)	1.239(2)	C(17)-Sn(1)-O(3)	88.83(6)	C(1)-O(1)-Sn(1)	122.76(10)
O(5)-H(5O)	0.79(3)	C(18)-Sn(1)-O(3)	86.78(6)	C(19)-O(5)-H(5O)	105.9(18)
N(1)-C(7)	1.303(2)	N(1)-Sn(1)-O(3)	70.07(5)	Sn(1)-O(5)-H(5O)	106.3(18)

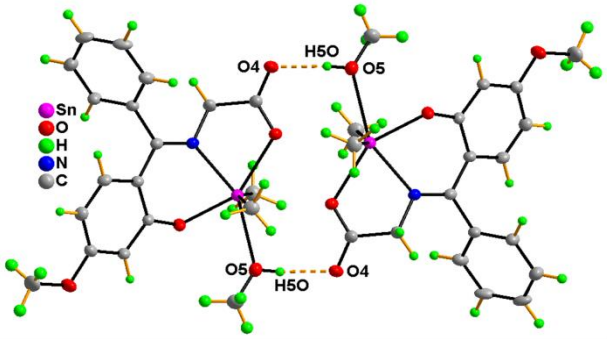

Fig. S7 Intermolecular hydrogen bonding pattern of **1-MeOH**.

C-H·····π interactions are encountered between benzophenone ring systems of neighbouring molecules with a distance of 2.79 Å, which produces a 1-D architecture along crystallographic b-axis shown in **Fig. S8**. In this architecture, the phenyl ring is oriented at an angle of 71.86° due to the edge to face C-H·····π interactions and are placed parallel to the phenyl rings in the neighbouring molecules at a distance of 3.76 Å and 4.20 Å.

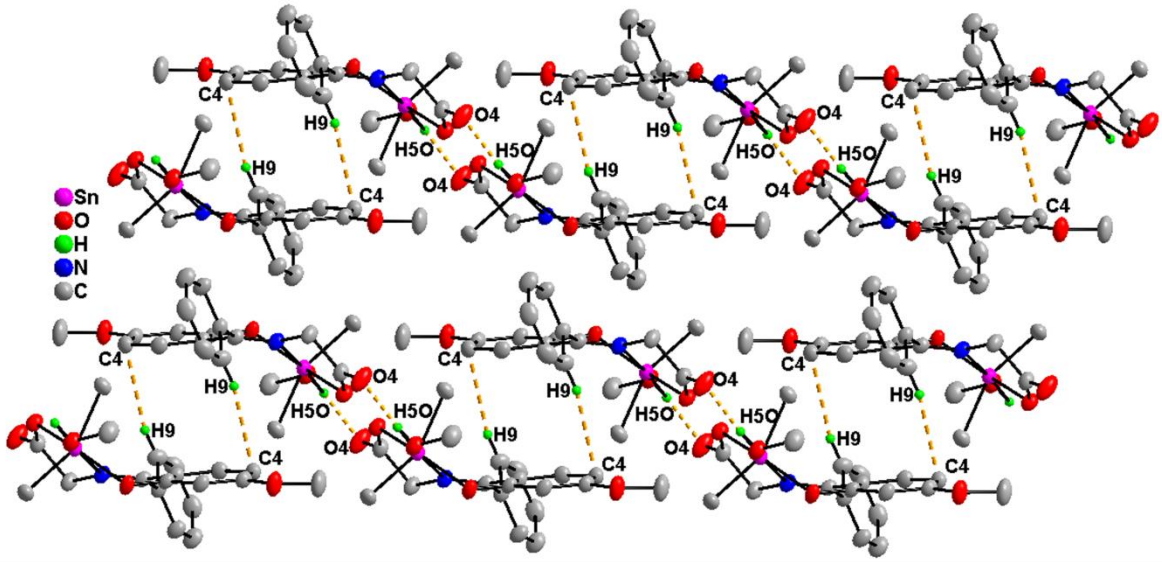

Fig. S8 C-H···π interactions in **1-MeOH** leading to 1-D chains.

Table S3: Selected bond lengths (Å) and bond angles (°) for **2′** and **3′**.

2′		**3′**	
Parameter	**X-ray Crystal Data**	**Parameter**	**X-ray Crystal Data**
Sn(1)-O(2) /Sn(4)-O(3)	2.005(4)/2.009(4)	Sn(1)-O(1)	2.020(4)
Sn(1)-C(2) /Sn(4)-C(8)	2.108(7)/2.112(6)	Sn(1)-C(2)	2.112(8)
Sn(1)-C(1) /Sn(4)-C(7)	2.111(6)/2.112(6)	Sn(1)-C(1)	2.129(9)
Sn(1)-O(11) /Sn(4)-O(7)	2.169(4)/2.170(4)	Sn(1)-O(3)	2.220(4)
Sn(1)-O(1) /Sn(4)-O(4)	2.194(4)/2.195(4)	Sn(1)-O(2)	2.214(4)
Sn(2)-O(2) /Sn(3)-O(3)	2.054(4)/2.050(4)	Sn(2)-O(1)	2.030(4)
Sn(2)-C(3) /Sn(3)-C(5)	2.106(7)/2.111(7)	Sn(2)-C(3)	2.141(9)
Sn(2)-C(4) /Sn(3)-C(6)	2.112(7)/2.116(6)	Sn(2)-C(4)	2.095(8)
Sn(2)-O(3) /Sn(3)-O(2)	2.144(4)/2.136(4)	Sn(2)-O(1)	2.123(4)
Sn(2)-O(1) /Sn(3)-O(4)	2.164(4)/2.163(4)	Sn(2)-O(2)	2.176(4)
O(11)-C(46) /O(7)-C(26)	1.296(6)/1.287(7)	O(3)-C(21)	1.291(8)
O(12)-C(46) /O(8)-C(26)	1.224(7)/1.224(7)	O(4)-C(21)	1.224(9)
O(2)-Sn(1)-C(2)/O(3)-Sn(4)-C(8)	114.8(3)/115.6(3)	O(1)-Sn(1)-C(2)	103.5(3)
O(2)-Sn(1)-C(1)/O(3)-Sn(4)-C(7)	116.6(3)/116.4(3)	O(1)-Sn(1)-C(1)	105.8(3)
C(2)-Sn(1)-C(1)/C(8)-Sn(4)-C(7)	127.4(3)/126.8(3)	C(2)-Sn(1)-C(1)	150.6(3)
O(2)-Sn(1)-O(11)/O(3)-Sn(4)-O(7)	81.51(15)/81.54(15)	O(1)-Sn(1)-O(3)	79.84(18)
C(2)-Sn(1)-O(11)/C(8)-Sn(4)-O(7)	99.6(3)/99.3(3)	C(2)-Sn(1)-O(3)	92.2(3)
C(1)-Sn(1)-O(11)/C(7)-Sn(4)-O(7)	97.7(3)/98.2(3)	C(1)-Sn(1)-O(3)	95.5(4)
O(2)-Sn(1)-O(1)/O(3)-Sn(4)-O(4)	72.35(16)/72.59(15)	O(1)-Sn(1)-O(2)	72.68(16)
C(2)-Sn(1)-O(1)/C(8)-Sn(4)-O(4)	92.8(3)/92.9(3)	C(2)-Sn(1)-O(2)	92.2(3)
C(1)-Sn(1)-O(1)/C(7)-Sn(4)-O(4)	92.7(3)/92.4(3)	C(1)-Sn(1)-O(2)	93.8(3)
O(11)-Sn(1)-O(1)/O(7)-Sn(4)-O(4)	153.82(15)/154.11(16)	O(2)-Sn(1)-O(3)	152.45(18)
O(2)-Sn(2)-C(3)/O(3)-Sn(3)-C(5)	109.3(2)/108.8(2)	O(1)-Sn(2)-C(3)	116.2(4)
O(2)-Sn(2)-C(4)/O(3)-Sn(3)-C(6)	110.7(2)/112.9(2)	O(1)-Sn(2)-C(4)	111.4(3)
C(3)-Sn(2)-C(4)/C(5)-Sn(3)-C(6)	140.0(3)/138.3(3)	C(4)-Sn(2)-C(3)	132.4(4)
O(2)-Sn(2)-O(3)/O(3)-Sn(3)-O(2)	74.11(14)/74.36(14)	O(1)-Sn(2)-O(1)#1	73.80(18)
C(3)-Sn(2)-O(3)/C(5)-Sn(3)-O(2)	95.1(2)/95.3(2)	O(1)#1-Sn(2)-C(3)	95.8(3)
C(4)-Sn(2)-O(3)/C(6)-Sn(3)-O(2)	94.6(2)/95.1(2)	C(4)-Sn(2)-O(1)#1	97.7(3)
O(2)-Sn(2)-O(1)/O(3)-Sn(3)-O(4)	72.09(14)/72.50(15)	O(1)-Sn(2)-O(2)	73.32(17)
C(3)-Sn(2)-O(1)/C(5)-Sn(3)-O(4)	96.3(3)/96.8(3)	C(3)-Sn(2)-O(2)	97.4(3)
C(4)-Sn(2)-O(1)/C(6)-Sn(3)-O(4)	96.7(3)/96.2(2)	C(4)-Sn(2)-O(2)	95.3(4)
O(3)-Sn(2)-O(1)/O(2)-Sn(3)-O(4)	146.20(14)/146.82(15)	O(1)#1-Sn(2)-O(2)	147.09(16)

Table S4 Intra- and intermolecular interactions; interatomic distance (Å) and bond angles (°) in compound **2′**.

Bond interactions (D–H···A)			D–H	H···A	D···A	D–H···A
Intra-molecular		N1–H1N···O5	0.877(79)	1.755(79)	2.558(6)	151.19(798)
		N2–H2N···O9	0.841(81)	1.779(79)	2.535(6)	148.70(817)
		C49–H49B···O12	0.988(6)	2.498(5)	3.166(8)	124.60(37)
Inter-molecular		C20–H20···O5	0.951(8)	2.428(4)	3.363(9)	167.92(44)
		C21–H21···O10	0.951(8)	2.393(5)	3.242(9)	148.53(50)
		C42–H42···O9	0.949(7)	2.375(4)	3.314(8)	147.26(42)

Apparently, the 2-D structure of compound **2′** shows a series of intra- and inter-molecular hydrogen bonds via weak to strong interactions (**Fig. S9**). The hydrogen bond lengths d(D-H), d(H···A), d(D···A), and angle (DHA) are given in **Table S4**. Ortho-substituted O5 and O9 are involved in bifurcated intra- (N1–H1N···O5 and N2–H2N···O9) and inter-molecular (C20–H20···O5 and C42–H42···O9) interactions. Furthermore, O10 is involved in intermolecular (C21–H21···O10) interactions, whereas O6 is not involved in any interactions leading to the generation of the non-centrosymmetric ladder type crystal structure.

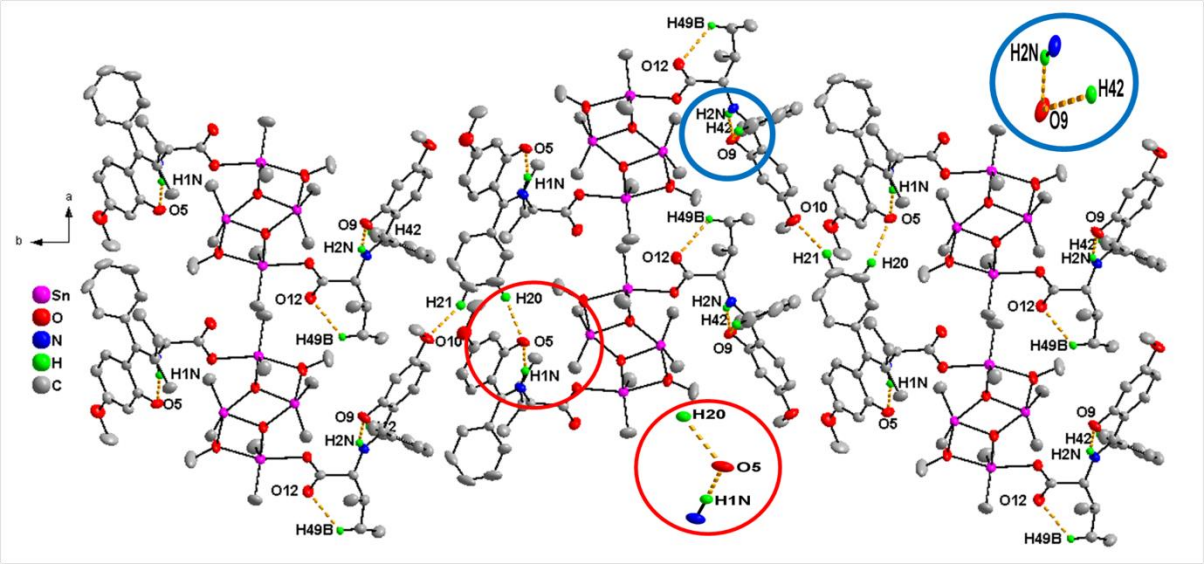

Fig. S9 The crystal packing of **2′** showing the intra- and intermolecular hydrogen bonding network. For clarity, H atoms that are not involved in hydrogen bonding have been omitted.

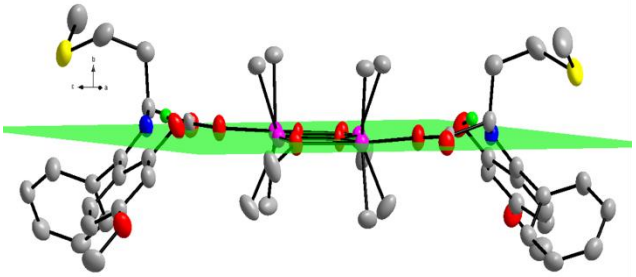

Fig. S10 View along the plane of the Sn_4O_4 core in the ladder-like compound **3′**.

Strong intermolecular interactions led to a 1-D architecture by virtue of intermolecular bonds (Sn1-O4* and Sn1*-O4). The extension of a one-dimensional network constructed a chain like structure equipped with a uniform distribution of 8-membered (2Sn, 4O, 2C) cage and tricyclic ladders.

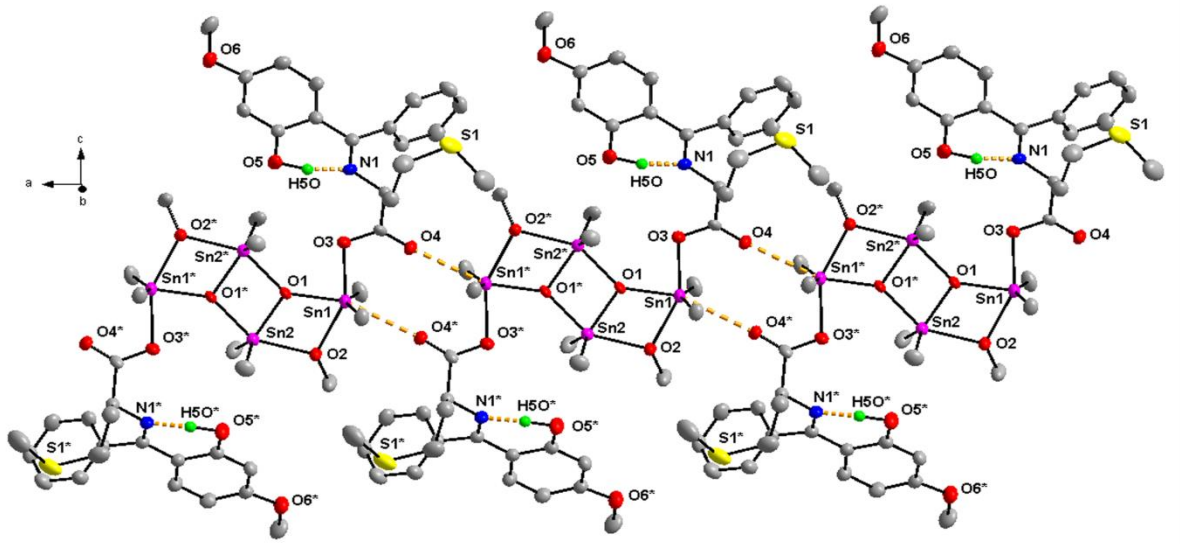

Fig. S11 The packing arrangement of molecules of **3′** viewed down the b axis. The dashed lines show H5O⋯N1 and H5O*⋯N1* hydrogen bonds and moderate coordinative interaction between Sn1-O4* and Sn1*-O4. Only H atoms involved in hydrogen bonds are shown.

4. Comparison of geometry for 1, 2′ and 3′

The **1·MeOH** has an extra coordination provided by the trans disposed nitrogen atom at sixth position of the coordination sphere of Sn. The average Sn-C distance is 2.101 Å in **1-MeOH** and is thus shorter as compared to the corresponding distances in pentacoordinate **2′** (2.111 Å) and **3′** (2.119 Å). The average Sn-O bond length is 2.342 Å in **1-MeOH** and hence

is longer than those found in related pentacoordinate **2′** (2.121 Å) and **3′** (2.131 Å). The C-Sn-C angles reflect the change from a pentacoordinate (126.8(3), 138.3(3), 140.0(3) and 127.4(3) for **2′**) and (150.6(3) and 132.4(4) for **3′**) to a hexacoordinated tin atom (152.32(8) for **1-MeOH**).

5. Fluorescence studies

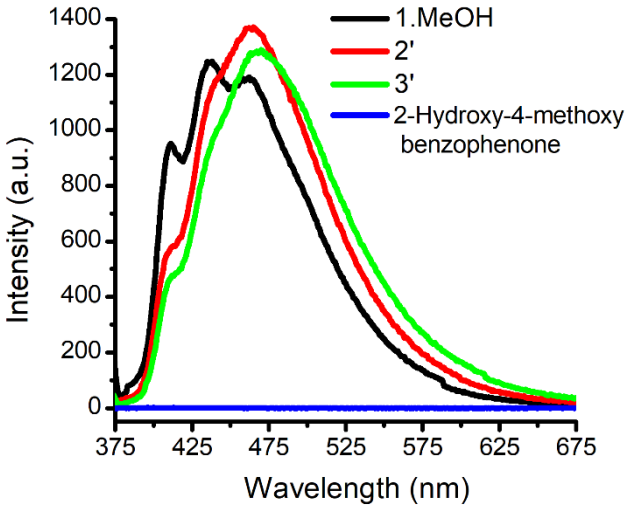

Fig. S12 Fluorescence emission spectra of methanolic solutions of **1** (0.19 mM, **2′** (0.07 mM), **3′** (0.07 mM) and 2-hydroxy-4-methoxybenzophenone (0.2 mM)

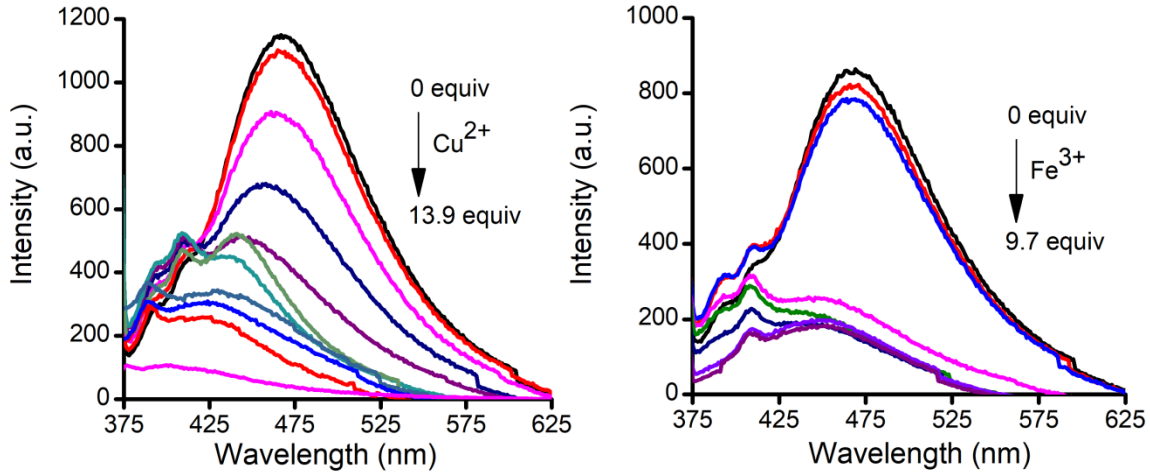

Fig. S13 Fluorescence emission of **3** (0. 14 mM) with the incremental addition of Cu^{2+} ions and **3** (0. 07 mM) with the incremental addition of Fe^{3+} ions

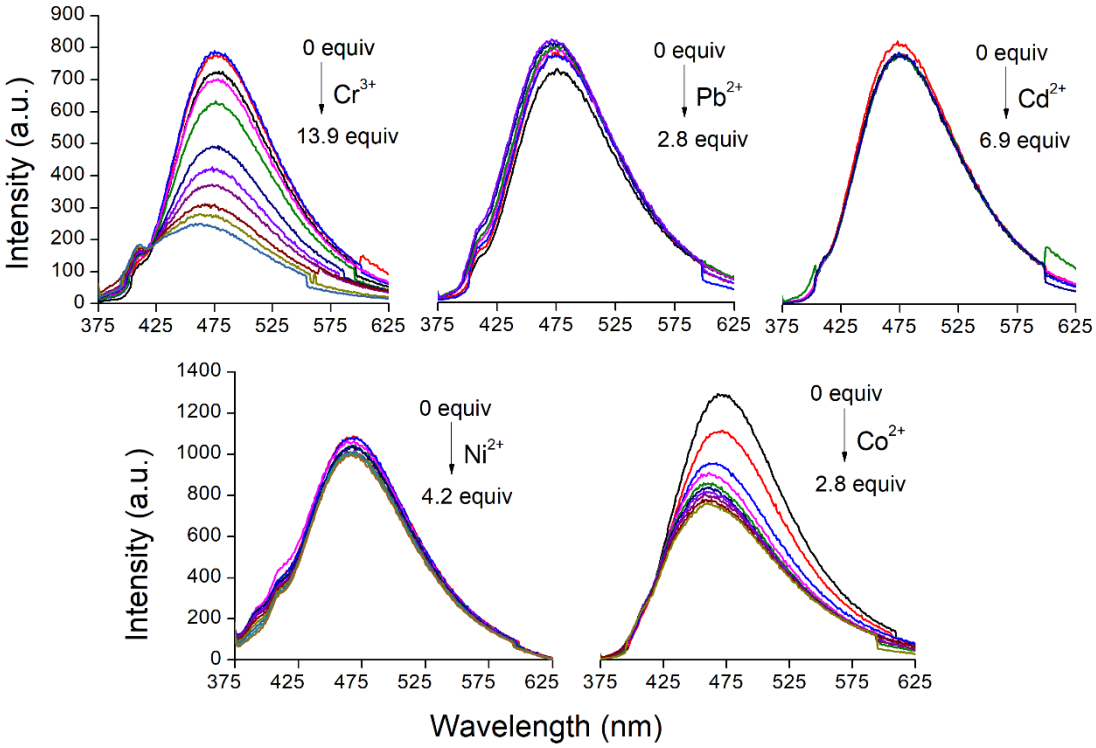

Fig. S14 Fluorescence emission spectra of **3** (0.07 mM) with incremental addition of Cr^{3+}, Pb^{2+}, Cd^{2+} and **3** (0.14 mM) with incremental addition of Co^{2+}, Ni^{2+} ions.

Quantum Yield

Quantum yield was calculated according to the following equation.

$$QY_x = QY_{ST}\frac{F_x}{F_{ST}}\frac{A_{ST}}{A_X}\frac{\eta_X^2}{\eta_{ST}^2}$$

F is the integral photon flux, *A* is the absorption factor, η is the refractive index of the solvent and *QY* is the quantum yield. The index *X* denotes the sample, and the index *ST* denotes the standard. Anthracene in ethanol was used as the reference (*QY* = 0.27).

Fluorescence Lifetime

Fluorescence life-time was calculated by using the following equation.

$$\text{Fluorescence life-time } (\tau) = (B_1T_1^2 + B_2T_2^2)/(B_1T_1 + B_2T_1)$$

Where B_1, B_2, T_1 and T_2 were parameters calculated from fitted fluorescence decay data for each individual system. The values of B_1, B_2, T_1 and T_2 are given below.

Compound	Parameters (B_1, B_2, T_1 and T_2)
1	$B_1 = 2.166259 \times 10^{-2}$, $B_2 = 6.644229 \times 10^{-4}$ $T_1 = 25.28073$, $T_2 = 133.1196$
2	$B_1 = 2.890307$, $B_2 = 2.204127 \times 10^{-2}$ $T_1 = 0.6716222$, $T_2 = 22.95243$
3	$B_1 = 1.177165 \times 10^{-2}$, $B_2 = 2.341968 \times 10^{-4}$ $T_1 = 26.4969$, $T_2 = 230.6804$
3 in the presence of Cu^{2+}	$B_1 = 8.904384 \times 10^{-2}$, $B_2 = 3.730271 \times 10^{-3}$ $T_1 = 24.96141$, $T_2 = 114.3369$
3 in the presence of Fe^{3+}	$B_1 = 0.8589792$, $B_2 = 1.518083 \times 10^{-2}$ $T_1 = 1.482797$, $T_2 = 24.36$

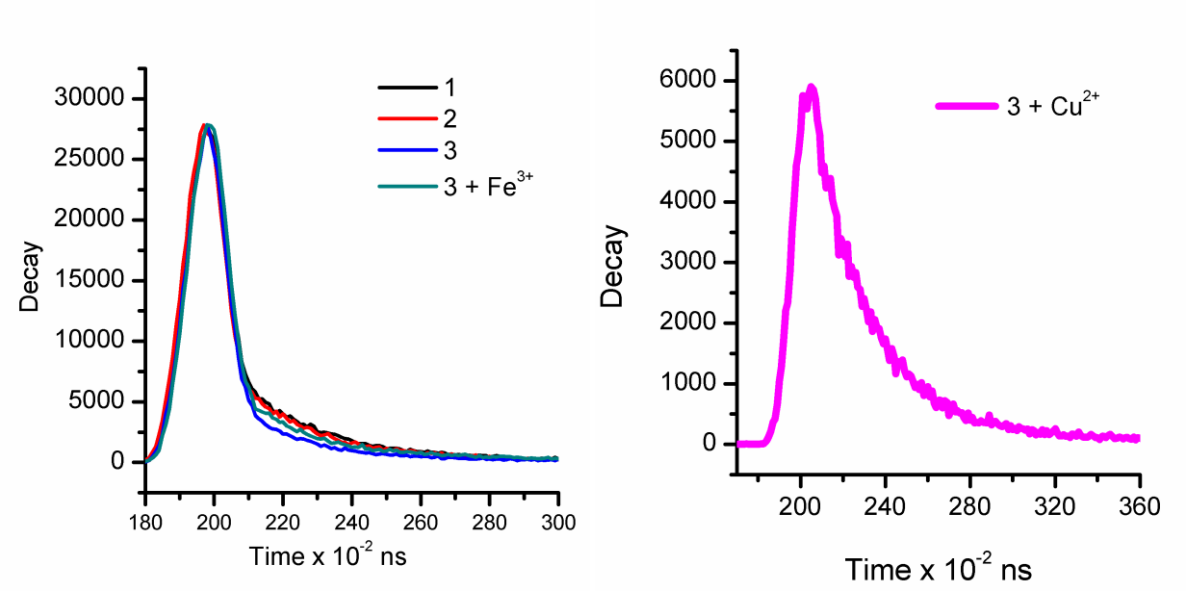

A B

Fig. S15 Fluorescence decay graphs of **1**-**3** and **3** in the presence of Fe^{3+} (A) and **3** in the presence of Cu^{2+} (B)

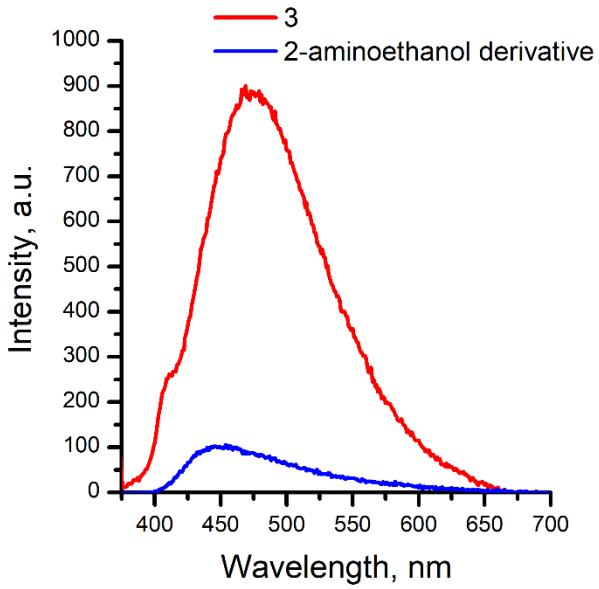

Fig. S16 Fluorescence emission spectra of **3** and its 2-aminoethanol analogue (100 µM) at excitation wavelength of 365 nm